NMR Investigation of Ionic Liquid−LiX Mixtures: Pyrrolidinium Cations and $TFSI^-$ Anions

Isabella Nicotera,[†] Cesare Oliviero,[†] Wesley A. Henderson,[‡,§] Giovanni B. Appetecchi,[‡] and Stefano Passerini[‡,*]

Department of Chemistry, University of Calabria, 87036-Arcavacata di Rende (CS) Italy, and ENEA (Italian National Agency for New Technologies, Energy and the Environment), IDROCOMB, Casaccia Research Centre, Via Anguillarese 301, 00060 Rome, Italy

Received: July 11, 2005; In Final Form: September 30, 2005

In this paper is reported an extensive NMR characterization of *N*-methyl-*N*-propyl-pyrrolidinium bis-(trifluoromethanesulfonyl)imide ($PYR_{13}TFSI$) room-temperature ionic liquid and its mixtures with LiTFSI. NMR was used to investigate the interactions between the ionic liquid and lithium salt and the diffusion coefficients of all ionic species present in these mixtures. The results are compared with previous DSC, Raman, and electrochemical investigations.

Introduction

Room-temperature ionic liquids (RTILs) are a rapidly expanding topic of research due to their favorable properties such as negligible volatility, high chemical, thermal, and electrochemical stability, high ionic conductivity, and, in some cases, hydrophobicity. These properties make them very attractive candidates for use in electrolytes for electrochemical applications such as the electrodeposition of electropositive metals, light-emitting electrochemical cells, photoelectrochemical cells, electrochemical capacitors, fuel cells, and batteries. Recently, we have shown that the addition of the RTIL $PYR_{13}TFSI$ strongly enhances the room-temperature ionic conductivity of solvent-free PEO-based polymer electrolytes.[1] Lithium metal batteries utilizing $P(EO)_{20}LiTFSI-PYR_{13}TFSI$ polymer electrolytes have excellent performance at temperatures as low as 313 K.[2] The long-term viability of RTILs as electrolytes for supercapacitors has also been demonstrated.[3] Utilizing RTIL−LiX mixtures may further improve the performance of supercapacitor electrolytes.

Although RTILs consist solely of ions, these ions are typically not electroactive in lithium batteries thus requiring the addition to the RTIL of a suitable LiX salt. In an effort to fully understand the properties of RTIL−LiX mixtures, we have extended our investigation of the phase behavior of $(1 - x)$ $PYR_{13}TFSI-(x)$ LiTFSI mixtures.[4] Preliminary work using differential scanning calorimetry (DSC) previously found that mixed salt crystalline phases form. A Raman investigation of the pure ionic liquid ($PYR_{13}TFSI$) and its 2:1 complex with LiTFSI was reported.[5] The ionic conductivity of pure $PYR_{13}TFSI$ and its mixtures with LiTFSI has also been investigated.[6] Here, we report a NMR investigation of $PYR_{13}TFSI$ and its mixtures with LiTFSI. The study was performed over a temperature range extending from 233 to 353 K, that is, with $PYR_{13}TFSI$ and its mixtures in both solid and liquid phases. The changes observed in the NMR spectra and calculated diffusion coefficients of ^1H, ^{19}F, and ^7Li with temperature and LiTFSI mole ratio (x) are correlated with the phase diagram and the ionic conductivity data. Only a few NMR studies of RTIL−LiX mixtures have been reported.[9−13] These investigations have been limited to relatively narrow composition and/or temperature ranges.

Experimental Section

Materials. The $PYR_{13}TFSI$ salt was prepared as previously reported.[4] $(1 - x)$ $PYR_{13}TFSI-(x)$ LiTFSI samples were also prepared as previously reported.[4]

Density Measurements. Density measurements were performed at different temperatures by weighing a known volume of sample fixed by using a calibrated volumetric flask (picnometer). The measurements were performed on the samples in the liquid phase, that is, in the temperature range from 293 to 353 K with the exception of the high melting point (mp) samples for which the temperature range was extended to 393 K. The temperature was typically changed in 20 K increments, and samples were equilibrated at each temperature for approximately 24 h. It is important to note that some mixtures were very difficult to crystallize. For example, the molten mixtures with $x = 0.33$, 0.40, and 0.50 do not crystallize for several days when stored at ambient temperature. The crystallization of these mixtures can be obtained only by slow cooling (10−20 °C day^{-1}). Overcooling these samples led to the formation of amorphous solids with very different physical properties as observed (in some cases) during NMR measurements.

NMR Measurements. NMR measurements were performed on a Bruker NMR spectrometer AVANCE 300 Wide Bore working at 300 MHz on ^1H, 116.6 MHz on ^7Li, and 282.4 MHz on ^{19}F, respectively. The employed probe was a Diff30 Z-diffusion 30 G/cm/A multinuclear with substitutable RF inserts: ^1H and ^{19}F with extended VT range (173 K, 473 K) and ^7Li with limited VT range (253 K, 333 K).

The ^1H and ^{13}C NMR high-resolution spectra (presented in Figure 1) were acquired at room temperature on a 7.4-T Bruker AC300 spectrometer. The samples (0.5−1.0 g each) were

* To whom correspondence should be addressed. Address: ENEA Via Anguillarese 301, 00060 Rome, Italy. Tel:+39 0630484985. E-mail: passerini@casaccia.enea.it.
[†] University of Calabria.
[‡] Casaccia Research Centre.
[§] Current address: Department of Chemistry, U. S. Naval Academy, 572 M Holloway Road (stop 9B), Annapolis, MD 21402.

10.1021/jp053799f CCC: $30.25
Published on Web 11/10/2005

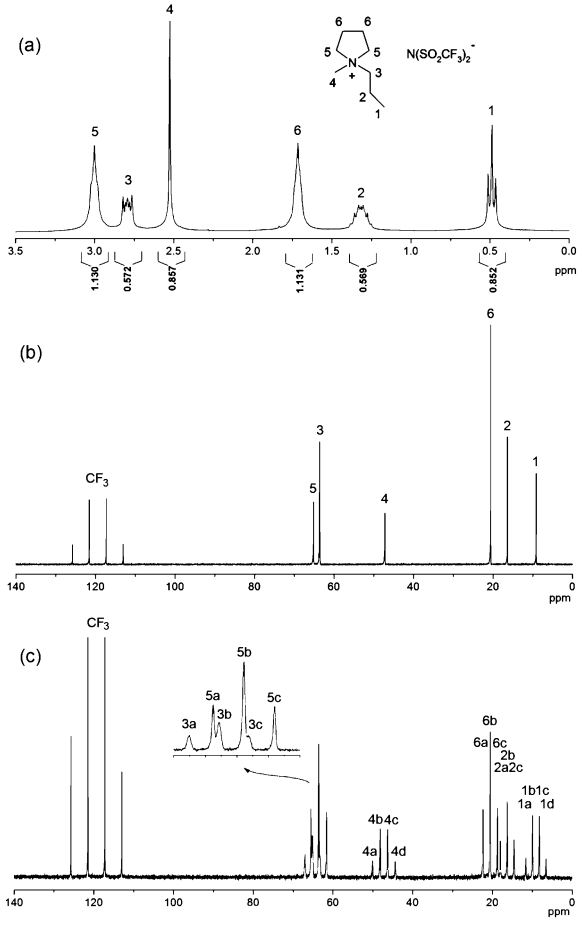

Figure 1. High-resolution (a) ^{1}H and ^{13}C, (b) decoupled, and (c) coupled NMR spectra of $PYR_{13}TFSI$. The peak assignments are indicated in the figure.

hermetically sealed in 5-mm Pyrex tubes in a glovebox. For reference purposes, a sealed capillary containing an aqueous solution of $LiCF_3SO_3$ was placed inside each Pyrex tube. The sealed sample tubes were first heated in an oven to 353 K and then slowly cooled to room temperature or placed in a freezer to aid in the crystallization of the high mp mixtures. In some cases, however, the samples appeared as solids but not fully crystallized. Samples were loaded into the NMR probe and slowly (1 K min^{-1}) cooled to 233 K.

^{1}H, ^{7}Li, and ^{19}F self-diffusion coefficients and spectra were taken at different temperatures. The temperature was changed at a slow rate (1 K min^{-1}) and equilibrated at each temperature for approximately 30 min. The spectra were obtained by applying the Fourier transform to the resulting free induction decay (FID) of a single $\pi/2$ pulse sequence.

The NMR pulsed field gradient spin−echo (PFG-SE) method[7] was used to measure the ^{7}Li and ^{19}F self-diffusion coefficients. This technique consists of two rf pulses, Hahn-echo sequence ($\pi/2-\tau-\pi$), with two identical magnetic field gradient pulses, the first applied between the 90° and 180° rf pulse (during the dephasing) and the second after the 180° rf pulse (during the rephasing) but before the echo. Following the usual notation, the magnetic field pulses have magnitude g, duration δ, and time delay Δ (different from the degree of ionic association). The attenuation of the echo amplitude is represented by the Stejskal−Tanner equation[7]

$$A(g) = \exp[-\gamma^2 g^2 D\delta^2(\Delta - (\delta/3))]$$

where D is the self-diffusion coefficient and γ is the nuclear gyromagnetic ratio. Note that the exponent in the equation is proportional to the mean-squared displacement of the molecules over an effective time scale ($\Delta - \delta/3$). For the investigated samples, the experimental parameters, Δ and δ, ranged from 40 to 80 and 5 ms, respectively, for ^{7}Li and from 60 to 80 and 2 ms, respectively, for ^{19}F. The gradient amplitude, g, varied from 100 to 800 G cm^{-1}.

For the ^{1}H self-diffusion coefficients measurements, we preferred to employ the pulsed field gradient stimulated echo (PFG-STE) method.[8] This sequence is generally applied when the materials are characterized by a transverse relaxation time (T_2) considerably shorter than longitudinal relaxation time (T_1), but in this case, the reason is purely related to the better quality of the obtained experimental data. The sequence consists of three 90° rf pulses ($\pi/2-\tau_1-\pi/2-\tau_m-\pi/2$) and two gradient pulses that are applied after the first and the third rf pulses, respectively. The echo is found at time $\tau = 2\tau_1 + \tau_m$. The echo amplitude is represented by the equation

$$I(2\tau_1 + \tau_m) = \frac{1}{2} I_0 \exp\left[-\frac{\tau_m}{T_1} - \frac{2\tau_1}{T_2} - (\gamma g\delta)^2 D\left(\Delta - \frac{\delta}{3}\right)\right]$$

thus, the diffusion coefficient is calculated in the same way as the PFG-SE method. The used experimental parameters were gradient pulse length $\delta = 5$ ms, time delay $\Delta = 80$ ms, and the gradient amplitude varied from 100 to 500 G cm^{-1}. The uncertainty in the self-diffusion measurements is ∼2%.

Results and Discussion

Figure 1 shows the high-resolution ^{1}H NMR and ^{13}C NMR spectra of $PYR_{13}TFSI$ at room temperature. The peak assignments were made on the basis of the chemical shifts and peak integrals of the ^{1}H spectrum and verified with the ^{13}C spectra. In particular, the ^{13}C−H coupling permits the easy observation of the multiplicities of the ^{13}C bands. The methyl ($-CH_3$) carbon atoms are split into quadruplets (carbons in the 1 and 4 positions), while the methylene ($-CH_2-$) carbons appear as triplets (carbons in the 2 and 6 positions). The group of signals appearing between 60 and 70 ppm (see magnification in the inset) is the result of two overlapping triplets. These signals result from the methylene carbons in positions 3 and 5 for which the neighboring nitrogen causes a small distortion of the peak shape. Finally, in both ^{13}C NMR decoupled and coupled spectra, the quadruplet resulting from the ^{13}C−^{19}F coupling of the anion $-CF_3$ groups is clearly observed. No unidentified peaks are observed in the ^{1}H and ^{13}C spectra.

In a previous work,[4] we have investigated the thermal properties of $(1 - x)$ $PYR_{13}TFSI-(x)$ LiTFSI mixtures. The phase diagram derived from the DSC measurements is illustrated in Figure 2. It was found that at least two crystalline complexes form with $x = 0.33$ and 0.67 (simply called 2:1 and 1:2) compositions and a eutectic is present at x values close to 0.15.

Typically, NMR spectra of solid phases are characterized by broad bands since dipolar and quadrupole interactions, chemical shifts, and scalar spin−spin coupling are substantially anisotropic, that is, depend on the orientation of the molecules with respect to the external magnetic field. In a rigid environment where the molecules have a very low mobility, the combination of all these effects results in the widening of the bandwidth. As materials approach their mp, the NMR bands narrow and become well defined in the molten state because the molecular tumbling motions become more rapid than the dipolar interaction strength, leading to time-averaged anisotropic contributions of zero.

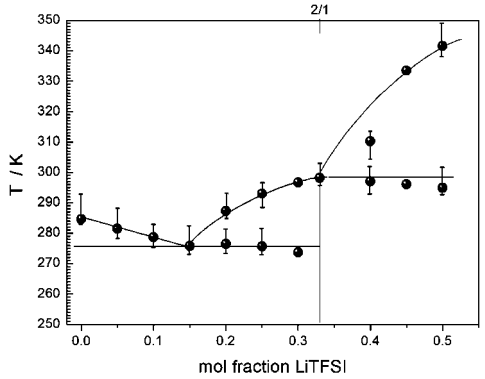

Figure 2. Phase diagram of the $(1 - x)$ $PYR_{13}TFSI-(x)$ LiTFSI mixtures. DSC data (solid dots) are taken from ref 4. The bars indicate the temperature intervals in which a phase transition is detected by ^{19}F NMR.

The ^{1}H spectra of the mixtures are reported in Figure 3. No external reference was used in these measurements. The ^{1}H peak position of the terminal protons in the propyl group (which are the farthest protons from the charged nitrogen and presumably the least influenced by experimental conditions) was therefore used as a reference and set to a value of 0 ppm.

The ^{1}H spectrum of the neat ionic liquid ($x = 0$) has broad lines at 273 K (in the crystalline state) (Figure 3). These lines become sharper at 283 K (just before the reported mp). At 288 K and higher (in the melt state), the spectra of the neat ionic liquid have a high resolution and it becomes possible to recognize the six multiplets observed in Figure 1. No changes are observed above 288 K except a further narrowing of the lines. The NMR transition temperatures agree very well with those observed by DSC (Figure 2). The $x = 0.20$ sample showed two phase transitions by DSC (Figure 2).[4] At 283 K (after the first transition), the lines narrow significantly as the neat $PYR_{13}TFSI$ portion of the sample melts. A further line narrowing is then observed at 296 K after the 2:1 complex melts in agreement with the phase diagram. The addition of LiTFSI to the $PYR_{13}TFSI$ results in large changes in the crystalline solid to melt transitions of the mixtures, but no substantial changes are observed in the peak position and shape of the ^{1}H spectra. This is to be expected since the PYR_{13}^{+} cations have only a weak interaction with the $TFSI^{-}$ anions and Li^{+} cations.

Figure 4 shows the ^{19}F NMR spectra for the samples. An internal reference (aqueous solution of $LiCF_3SO_3$ sealed in a capillary placed inside the NMR tube) was used in these measurements, and all chemical shifts are reported with respect to the position (0 ppm) of the ^{19}F peak of the reference material. At 353 K, the ^{19}F spectra for all of the samples consist of a single narrow peak indicating that all the fluorines in the $TFSI^{-}$ anions are equivalent in the melt on the time scale of the NMR experiment. The ^{19}F peak of the samples, however, shows multiple components at temperatures below the mp. In addition, the ^{19}F peak shifts in the negative direction as the lithium content increased (from about -1.42 ppm at $x = 0$ to about -1.8 ppm at $x = 0.50$) indicating that the anions in the melt interact strongly with the Li^{+} cations.

With decreasing temperature, there is no appreciable change in the chemical shift of the neat $PYR_{13}TFSI$ ($x = 0$) ^{19}F peak (Figure 4). A shift is observed, however, when the sample is crystalline. The sharp peak in the 283 K spectrum is due to the onset of melting. The samples with LiTFSI in the melt do have a negative shift of the ^{19}F peak with increasing temperature. The $x = 0.33$ sample shows a net peak narrowing in a very small temperature interval from 296 to 303 K. This is in very

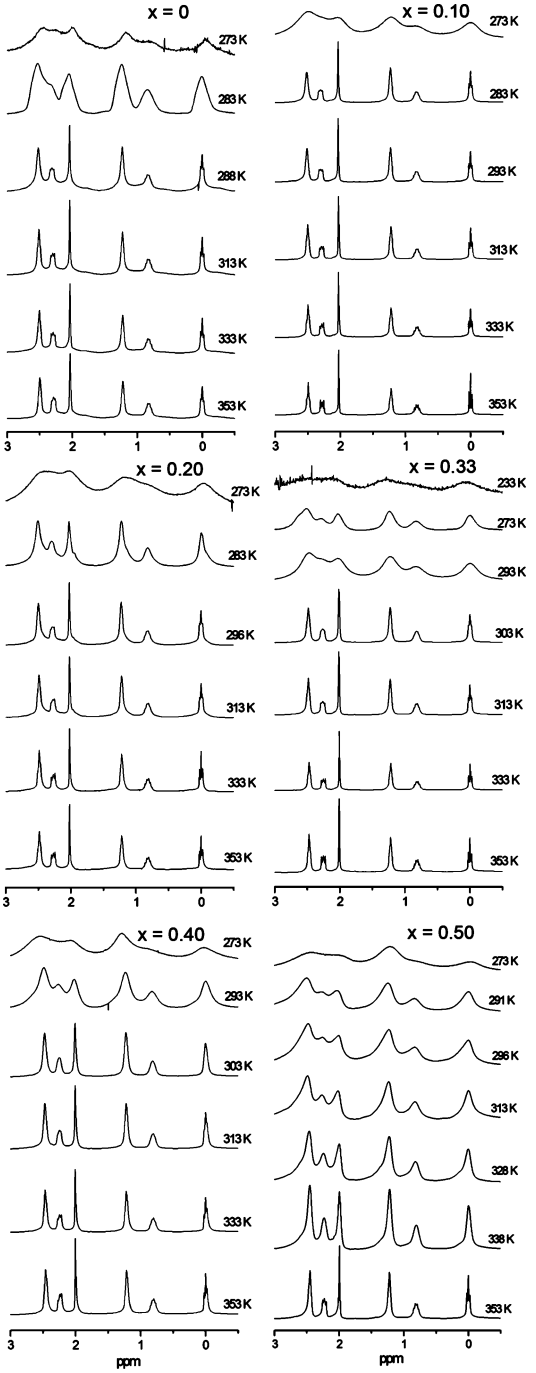

Figure 3. ^{1}H NMR spectra of $(1 - x)$ $PYR_{13}TFSI-(x)$ LiTFSI mixtures as a function of temperature.

good agreement with the ^{1}H NMR results illustrated above and previous DSC measurements,[4] which have shown that the 2:1 crystalline complex melts in a single step. The sample with $x = 0.50$, however, shows two components in the ^{19}F spectrum at 292 K. The peak splitting in the solid phase at a temperature slightly below the first mp may be attributed to the different environments of the anions in the 2:1 and 1:2 crystalline complexes. The thermal energy available could be enough to activate the spinning of the terminal $-CF_3$ groups in the soft anion leading to a partial differentiation of the fluorines. At 303 K, that is, when the 2:1 crystalline complex is in the molten state, the peak appears narrower but a broader component is still observed by peak fitting. At this temperature, the presence of two peaks is due to the coexistence of a 2:1 melt phase (narrow peak) and solid 1:2 phase (broad peak). The predomi-

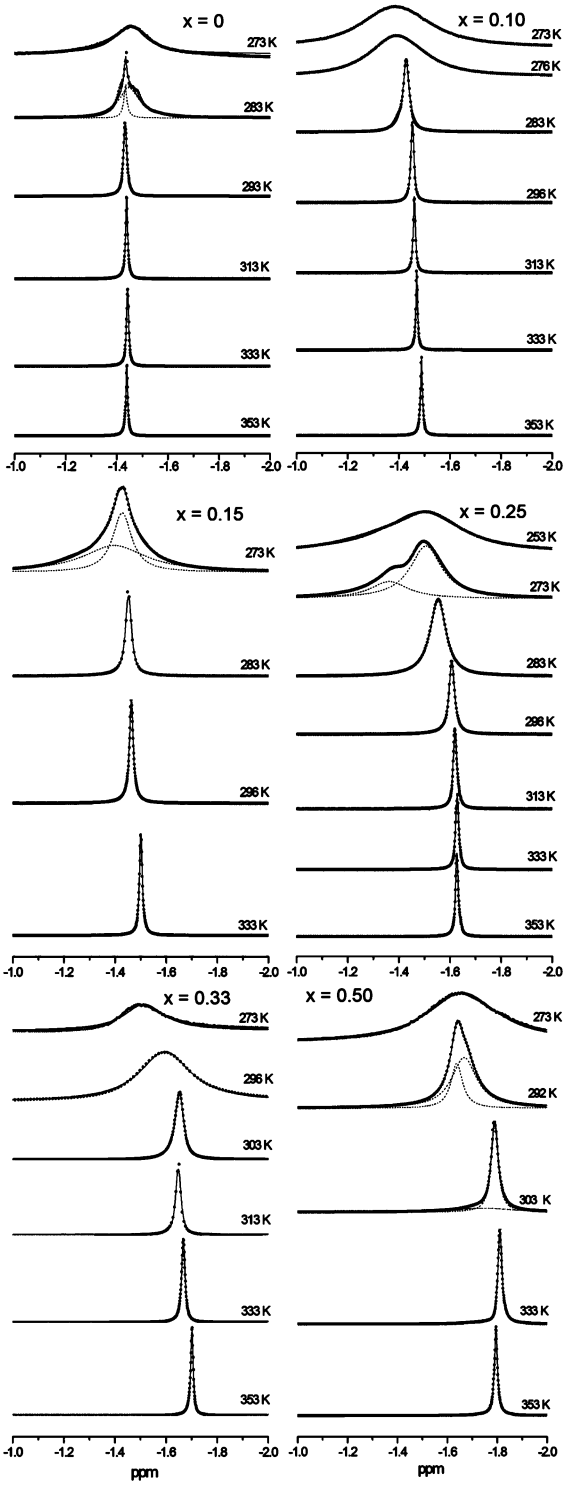

Figure 4. ^{19}F NMR spectra of $(1 - x)$ $PYR_{13}TFSI-(x)$ LiTFSI mixtures as a function of temperature.

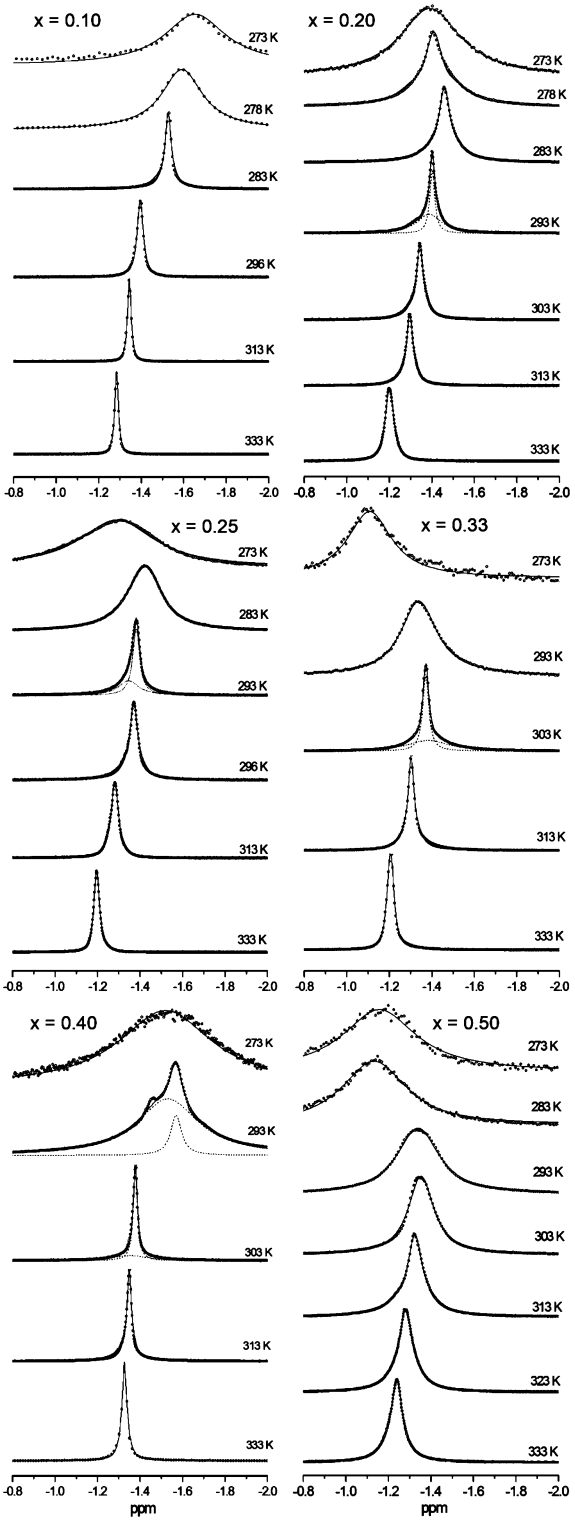

Figure 5. ^{7}Li NMR spectra of $(1 - x)$ $PYR_{13}TFSI-(x)$ LiTFSI mixtures as a function of temperature.

nance of the liquid phase peak is fictitious because the areas of both peaks are comparable. At 333 K, the peak is narrower, but it still shows an asymmetric shape that reveals the presence of the broader peak. However, at 353 K, the peak becomes very narrow and symmetric in shape as expected for a fully homogeneous liquid phase, in complete agreement with previous DSC results.[4]

As there is no solvent present in these mixtures, the Li^+ cations are likely to be coordinated by oxygens from multiple $TFSI^-$ anions.[14−16] In the 2:1 crystalline complex, there are three $TFSI^-$ anions present for each Li^+ cation. Figure 5 shows the ^{7}Li NMR spectra for the samples. The reference for the chemical shifts is the same as that used for the ^{19}F spectra. For some of the samples, as the 2:1 crystalline complex melts, the ^{7}Li peaks shift to lower ppm values. Thereafter, the ^{7}Li peaks shift to higher ppm values with increasing temperature. The ^{7}Li peak shape of the samples with $x \geq 0.33$ at low temperature (273 K and lower) shows a single, but very broad, peak typical of a solid phase. As the temperature increases to 293 K, the samples still show a broad peak, however, the $x = 0.40$ sample also displays two narrower peaks. These two peaks most likely

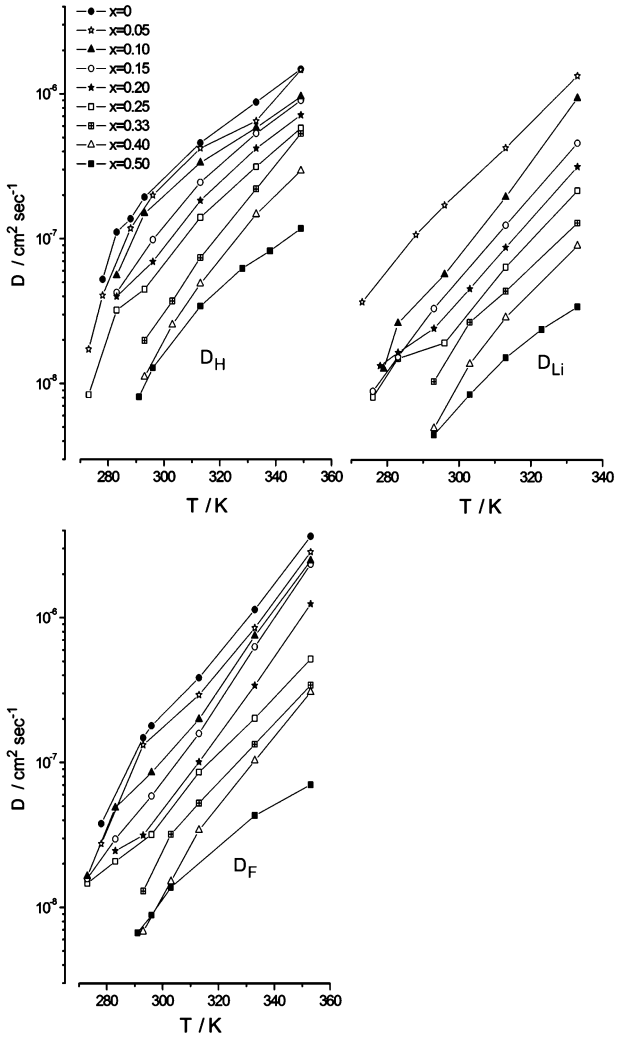

Figure 6. Self-diffusion coefficients (D_H, D_F, and D_{Li}) of $(1 - x)$ $PYR_{13}TFSI-(x)$ LiTFSI mixtures as a function of temperature.

originate from the melting of an amorphous solid phase. The $x = 0.40$ mixture is the most difficult to crystallize (a molten sample left on the benchtop did not solidify in four weeks). At 303 K, that is, above the mp of the 2:1 crystalline complex, the three mixtures with $x \geq 0.33$ showed a substantial narrowing of the ^{7}Li peak. The peak remains substantially broader for the $x = 0.50$ sample for which spectra in the fully molten state could not be recorded because the maximum temperature of the ^{7}Li probe used was 333 K.

To investigate the ionic conduction processes in the samples, ^{1}H, ^{7}Li, and ^{19}F self-diffusion coefficients were measured at different temperatures by means of the pulsed field gradient (PFG) NMR method. Two different sequences (see Experimental section) were used: ^{1}H (pulsed field gradient stimulated echo, PFG-STE) and ^{7}Li and ^{19}F (pulsed field gradient spin−echo, PFG-SE). The D_H, D_F, and D_{Li} values are shown in Figure 6. The self-diffusion coefficients reached values as high as 2×10^{-6}, 4×10^{-6}, and 1.5×10^{-6} cm^2 s^{-1}, respectively, for the PYR_{13}^+ cation, $TFSI^-$ anion, and Li^+ cation, depending on the composition of the mixtures. The lower limit for all nuclei was fixed by the detection limit of the system in the range of 4×10^{-9} to 8×10^{-9} cm^2 s^{-1}.

The self-diffusion coefficients increase with increasing temperature, as expected (Figure 6). The mixtures with $x \geq 0.33$ show reliable values of D_H, D_F, and D_{Li} only at temperatures above 293 K (where a mixed liquid−solid-phase exists), while

TABLE 1: σ_{NMR} (σ_{obs}) Ionic Conductivity Values (mS cm^{-1}) of $(1 - x)$ $PYR_{13}TFSI-(x)$ LiTFSI Mixtures

x	283K	293 K	313 K	333 K
0		4.52 (2.75)	10.3 (4.65)	23.0 (6.42)
0.05		4.06 (2.41)	8.99 (4.80)	17.9 (8.02)
0.10	1.50 (1.08)	2.67 (1.74)	6.59 (3.59)	19.2 (5.83)
0.15		1.87	3.02	14.2
0.20	0.923	1.28	3.62	9.34
0.25	0.775 (0.257)	1.03 (0.532)	2.93 (1.80)	6.48 (3.78)
0.33		0.466 (−)	1.72 (0.856)	4.46 (2.12)
0.40		0.260 (−)	1.17 (0.436)	3.29 (1.22)
0.50				1.48 (0.204)

the mixtures with $x \leq 0.25$ show reliable D values at 273−283 K. Above 293 K, the D values increase at approximately the same rate independent of the salt mixture composition with the exception of the sample with $x = 0.50$ which shows a lower increase of D_H, D_F, and D_{Li} with temperature (especially at higher temperatures). This trend agrees very well with the phase changes identified by DSC and confirmed above by NMR. The D_H, D_F, and D_{Li} self-diffusion coefficients decrease with increasing LiTFSI molar ratio (x) in full agreement with the decrease in conductivity observed as the LiTFSI mole fraction increases.[6] The decrease in the PYR_{13}^+ mobility as the LiTFSI mole fraction increases is likely due to the interaction of the $TFSI^-$ counterions with the Li^+ cations constraining the organic cations by fixed electrostatic interactions and reduced free volume. For all of the samples over the entire temperature range, $D_F > D_{Li}$ indicating that the $TFSI^-$ anions have greater mobility than the Li^+ cations.

The conductivity of the samples previously reported (σ_{obs})[6] is compared to conductivity values calculated from the D_H, D_F, and D_{Li} self-diffusion coefficients obtained by PFG-NMR (σ_{NMR}) in Table 1. The ionic conductivity of the mixtures was calculated from the self-diffusion coefficients using the Nernst−Einstein equation

$$\sigma = e^2(N_H D_H + (N_H + N_{Li})D_F + N_{Li}D_{Li})/(kT)$$

where N_H and N_{Li} are the number of ions per unit volume ($N_H = (1 - x)N_A/V_M$, $N_{Li} = xN_A/V_M$), with V_M (molar volume) being given by the ratio of the sample composite molecular mass ($(1 - x)MW_{PYR13TFSI} + (x)MW_{LiTFSI}$) and density. The composite molecular mass, density, and molar volume of the samples at different temperatures are given in Table 2. The calculated conductivity values are always higher than the experimental values. This deviation may be explained in terms of the validity of the Nernst−Einstein equation being applied to the system under study. The premise of the Nernst−Einstein equation is that of unbounded motion within a single-phase medium. Clearly, from the difference between the measured and calculated conductivities, this is not the case for the samples. The simplest explanation of this discrepancy is the presence of mobile ion pairs which contribute to the spin−echo decay in the PFG-SE experiment, but do not result in a net charge transport. A previous study of the ionic conductivity and the self-diffusion coefficients in electrolytes composed of LiTFSI dissolved in γ-butyrolactone and propylene carbonate also reported that the ionic conductivities calculated from the NMR self-diffusion coefficients (σ_{NMR}) were substantially higher than the measured ones (σ_{obs}).[17] The calculated degree of ionic association (Δ)[18] defined as $\Delta = 1 - (\sigma_{obs}/\sigma_{NMR})$ ranged from 0.45 to 0.65, depending upon the solvent and the salt concentration.[17] The calculated Δ values for the samples studied here are reported in Table 3. The results indicate that Δ generally increases with increasing temperatures. These results are

TABLE 2: Composite Molecular Weight (amu), Density (ρ) (g cm^{-3}), and V_M (cm^3) of (1 − x) $PYR_{13}TFSI$−(x) LiTFSI Mixtures as a Function of Temperature and LiTFSI Mole Fraction[a]

	MW	277 K		293 K		313 K		333 K		353 K		373 K		393 K	
x	(amu)	ρ	V_M	ρ	V_M	ρ	V_M	ρ	V_M	ρ	V_M	ρ	V_M	ρ	V_M
0	408.38			1.411	289.43	1.399	291.91	1.386	294.65	1.369	298.31				
0.05	402.32			1.425	282.33	1.414	284.52	1.397	287.98	1.382	291.11				
0.10	396.25	1.474	268.83	1.456	272.15	1.441	274.98	1.420	279.05	1.407	281.63				
0.15	390.19			1.469	265.61	1.451	268.91	1.435	271.91	1.419	274.97				
0.20	384.12	1.500	256.08	1.490	257.80	1.465	262.20	1.444	266.01	1.436	267.49				
0.25	378.06	1.523[b]	248.23	1.510	250.37	1.493	253.22	1.479	255.62	1.458	259.30				
0.33	368.35			1.510*	243.94	1.522	242.02	1.506	244.59	1.488	247.55	1.473	250.07		
0.40	359.86			1.583[b]	227.33	1.572[c]	228.92	1.549	232.32	1.530	235.20	1.512	238.00	1.494	240.87
0.50	347.73							1.589**	218.84	1.547	224.78	1.532	226.98	1.512	229.98

[a] The experimental error on the density measurements is lower than ±0.005 g cm^{-3}. [b] Mostly solid phase with large crystals. [c] Mixed liquid and solid phases.

TABLE 3: Degree of Ionic Association (Δ) of (1 − x) $PYR_{13}TFSI$−(x) LiTFSI Mixtures Calculated at Selected Temperatures

x	Δ (283 K)	Δ (293 K)	Δ (313 K)	Δ (333 K)
0		0.39	0.55	0.72
0.05		0.41	0.47	0.55
0.10	0.28	0.35	0.46	0.65
0.25	0.67	0.49	0.39	0.42
0.33		1.00	0.50	0.52
0.40		1.00	0.63	0.63
0.50				0.86

somewhat counterintuitive since the Li^+ cations are likely to be highly aggregated over the entire temperature and composition range. One explanation for this may be that the Nernst−Einstein equation is not appropriate for describing conductivity in this system. In the absence of an electric field, a mobile ion will perform a random walk. When an electric field is applied, the ion will migrate toward the oppositely charged electrode but, this migration is superimposed upon the random walk movement of the ion from thermal energy. Diffusion NMR measures random (Brownian) motion of ions, including correlated ones (i.e., ion pairs), while σ measures only the net charge transport in the presence of an electric field. Thus, the calculated conductivity values from self-diffusion coefficients can always be expected to be higher than observed ac or dc conductivity measurements.

Conclusions

In summary, we have conducted an extensive NMR investigation of (1 − x) $PYR_{13}TFSI$−(x) LiTFSI mixtures. The results of the NMR investigations are compared with previous Raman, DSC, and ionic conductivity studies. The evolution of the ^1H, ^{19}F, and ^7Li NMR spectra with varying temperature and composition has confirmed the phase diagram proposed in a previous work,[4] identifying the existence of a crystalline complex at $x = 0.33$ and a eutectic at x close to 0.15. The ^1H, ^{19}F, and ^7Li self-diffusion coefficients were obtained by the PFG-NMR method, and the results are discussed. This investigation indicates that RTIL−LiX salt mixtures are promising candidates for electrochemical applications since the nonvolatile, thermally stable RTIL is a viable replacement for molecular solvents in liquid electrolytes for high-energy lithium batteries and hybrid supercapacitors.

Acknowledgment. W.A.H. is indebted to the National Science Foundation for a research fellowship (International Research Fellowship Program 0202620). The financial support of the Italian Ministry of University Research (MIUR) is also kindly acknowledged. Any opinions, findings, and conclusions or recommendations expressed in this material are those of the authors and do not necessarily reflect the views of the National Science Foundation.

References and Notes

(1) Shin, J.-H.; Henderson, W. A.; Passerini, S. *Electrochem. Commun.* **2003**, *5*, 1016.
(2) Shin, J.-H.; Henderson, W. A.; Passerini, S. *Electrochem. Solid-State Lett.* **2005**, *8*, A125.
(3) Balducci, A.; Henderson, W. A.; Mastragostino, M.; Passerini, S.; Simon, P.; Soavi, F. *Electrochim. Acta* **2005**, *50*, 2233.
(4) Henderson, W. A.; Passerini, S. *Chem. Mater.* **2004**, *16*, 2881.
(5) Castriota, M.; Caruso, T.; Agostino, R. G.; Cazzanelli, E.; Henderson, W. A.; Passerini, S. *J. Phys. Chem. A* **2005**, *109*, 92.
(6) Henderson, W. A.; Shin, J.-H.; Edmondson, C.; De Long, H. C.; Trulove, P. C.; Passerini, S. *Chem. Mater.*, in preparation.
(7) Stejskal, E. O.; Tanner, J. E. *J. Phys. Chem.* **1965**, *42*, 288.
(8) Tanner, J. E. *J. Chem Phys.* **1970**, *52*, 2523.
(9) Fung, Y. S.; Chau, S. M. *Inorg. Chem.* **1995**, *34*, 2371.
(10) Forsyth, M.; Huang, J.; MacFarlane, D. R. *J. Mater. Chem.* **2000**, *10*, 2259.
(11) MacFarlane, D. R.; Forsyth, M. *Adv. Mater.* **2001**, *13*, 957.
(12) Efthimiadis, J.; Annat, G. J.; Efthimiadis, J.; Forsyth, M.; MacFarlane, D. R. *Phys. Chem. Chem. Phys.* **2003**, *5*, 5558.
(13) Hayamizu, K.; Aihara, Y.; Nakagawa, H.; Nukuda, T.; Price, W. S. *J. Phys. Chem. B* **2004**, *108*, 19527.
(14) Nowinski, J. L.; Lightfoot, P.; Bruce, P. G. *J. Mater. Chem.* **1994**, *4*, 1579.
(15) Brouillette, D.; Irish, D. E.; Taylor, N. J.; Perron, G.; Odziemkowski, M.; Desnoyers, J. E. *Phys. Chem. Chem. Phys.* **2002**, *4*, 6063.
(16) Henderson, W. A.; McKeena, F.; Khan, M. A.; Brooks, N. R.; Young, V. G., Jr.; Frech, R. *Chem. Mater.* **2005**, *17*, 2284.
(17) Aihara, Y.; Arai, S.; Hayamizu, K. *Electrochim.* Acta **2000**, *45*, 1321.
(18) Payne, W. A.; Forsyth, M.; Ratner, M. A.; Shriver, D. F.; de Leeuw, S. W. *J. Chem. Phys.* **1994**, *100* 5201.